Calculations of rates for strong-field ionization of alkali-metal atoms in the quasistatic regime

M. Z. Milošević
Faculty of Science and Mathematics, University of Niš, Višegradska 33, 18000 Niš, Serbia

N. S. Simonović
Institute of Physics, University of Belgrade, P.O. Box 57, 11001 Belgrade, Serbia

(Received 13 January 2015; published 20 February 2015)

Tunneling and over-the-barrier ionization of alkali-metal atoms in strong electromagnetic fields are studied using the single-electron model (valence electron plus atomic core) and the frozen-core approximation. The lowest-state energies and widths (ionization rates) at different values of applied field, obtained using the Stark shift expansion and the Ammosov-Delone-Krainov formula, respectively, are compared with the corresponding values determined numerically by the complex rotation method. Good agreement for the energies is obtained at the field strengths corresponding to the tunneling regime. In contrast, the rates obtained by the Ammosov-Delone-Krainov formula significantly overestimate numerical results. After introducing a correction in the formula that accounts for the dependence of the binding energy on the field strength, good agreement in the tunneling regime is obtained for the rates too. A disagreement that still remains in the over-the-barrier ionization regime indicates that at stronger fields further corrections of the rate formula, such as those related to the form of the bound-state wave function, are required. Finally, it is demonstrated that numerically determined ionization rates are not too sensitive to the choice of model for the effective core potential and good results can be obtained using a simple local pseudopotential.

DOI: 10.1103/PhysRevA.91.023424 PACS number(s): 32.80.Fb, 32.80.Rm, 32.90.+a

I. INTRODUCTION

Atoms and molecules, when exposed to high-intensity laser fields, exhibit a variety of interesting phenomena related to the field-induced ionization including the above threshold ionization (ATI), high-harmonic generation, atomic stabilization, nonsequential double ionization, dissociative ionization, etc. (For a review of progress in the physics of strong-field atomic processes see, e.g., Ref. [1] and references therein.) From the theoretical point of view, a common feature for all of these phenomena is that they cannot be described perturbatively. A perturbative treatment is in principle applicable in the case of single- or few-photon processes. Namely, a single photon with the energy $\hbar\omega$, which is larger than the ionization potential I_p of an atom ($\hbar\omega > I_p$), is enough to ionize this atom. The ionization rate is therefore large even at very low intensities. In this case the term describing the atom-field interaction in the full Hamiltonian can be treated as a perturbation for the unperturbed atomic Hamiltonian. This treatment is generalized to multiphoton processes, but it is not applicable at sufficiently large intensities. One indication of the nonperturbative regime is just the ATI, in which the atom absorbs more photons than the minimum required.

At even larger intensities, the field becomes comparable to the atomic potential, opening up another ionization mechanism: the tunnel ionization. In this case the field distorts the atomic potential forming a potential barrier through which the electron can tunnel. Finally, at the highest intensities, the field strength overcomes the atomic potential. This can be considered as the limiting case of tunnel ionization when the barrier is suppressed below the energy of atomic state. This regime is usually referred to as over-the-barrier ionization (OBI). The transition from the multiphoton to the tunneling regime is governed by the Keldysh parameter [2]

$$\gamma = \frac{\omega\sqrt{2I_p}}{F}, \tag{1}$$

where F is the peak value of the electric component of electromagnetic field. (For the sake of simplicity hereafter we use the atomic system of units: $e = m_e = \hbar = 4\pi\varepsilon_0 = 1$.) If $\gamma \ll 1$ (low-intensity–short-wavelength limit) tunnel ionization dominates, whereas for $\gamma \gg 1$ (high-intensity–long-wavelength limit) multiphoton ionization does. An overview of different strong-field ionization regimes can be found, e.g., in Ref. [3].

Tunnel ionization is successfully described by the Ammosov-Delone-Krainov (ADK) semiclassical theory [4]. The starting point of the theory is the quasistatic approximation, which assumes that for $\gamma \ll 1$ the electric field changes slowly enough that a static tunneling rate can be calculated for each instantaneous value of the field. The tunneling rate for the alternating field of a frequency ω then can be obtained by averaging the static rates over the field period $2\pi/\omega$. The ADK theory accurately predicts tunneling rates in experiments with atomic ionization in strong fields [5,6]. It also shows excellent agreement with exact numerical calculations in the low-field limit of the tunneling regime, i.e., for field strengths much below the OBI domain (for hydrogen and helium see Refs. [7,8]).

However, for atoms with low ionization potentials, as in the case of alkali-metal atoms, the OBI regime begins at much lower values of the field strength than for hydrogen or noble gases. For example, the laser peak intensity that corresponds to the OBI threshold for rubidium is about 1.5×10^{12} W/cm^2, whereas the corresponding value for hydrogen atom is two orders of magnitude larger, $\approx 1.5 \times 10^{14}$ W/cm^2 (see Sec. II B). The tunneling regime for alkali-metal atoms is therefore

reduced to a short interval of relatively-low-field strengths and the applicability of the ADK theory for these atoms might be limited. This question, as well as the simple electronic structure of alkali-metal atoms, inspired the study presented in this paper. In the next section we introduce a single-electron model for alkali-metal atoms (valence electron plus atomic core) and study the strong-field ionization regimes (tunneling and OBI) in the quasistatic approximation. In the same section we consider a correction to the ADK rate formula for atoms with low ionization potentials. The effective core potential models and the calculation technique (the complex rotation method), used to obtain numerical results, are described in Sec. III and the Appendixes. In Sec. IV we present numerical results (the lowest-state energies and ionization rates) for the alkali-metal atoms and compare them with the results obtained using the Stark shift expansion and the corrected ADK formula. Section V contains a summary and conclusions.

II. MODEL AND ANALYTICAL ESTIMATIONS

A. Single-electron model and frozen-core approximation

Many properties of alkali-metal atoms depend mainly on the dynamics of the valence electron. This follows from the structure of these atoms, which is that of a single valence electron moving in an orbital outside a core that consists of closed (sub)shells. In this case the total orbital momentum and spin of the core are equal to zero and the core is spherically symmetric. Thus, the valence electron of a neutral alkali-metal atom moves in an effective core potential (ECP) $V_{\rm core}(r)$, which at large distances r approaches the Coulomb potential $V_C = -1/r$ (the nuclear charge Z is then screened by $Z-1$ core electrons) [see Fig. 1(a)]. Compared to the core electrons, the valence electron is weakly bound. This fact explains many properties of alkali-metal atoms such as the optical spectrum, which is determined by the transitions involving the valence electron only. The lowest state of the valence electron has zero orbital angular momentum ($l=0$) and the corresponding orbital can be designated by $n_0 s$, where n_0 is the lowest value of the principal quantum number n of this electron ($n_0 = 2$ for Li, 3 for Na, 4 for K, etc.). The energy levels of the valence electron of the alkali-metal atom can be represented by the Rydberg-like formula $E_{nl} = -1/2n^{*2}$, where $n^* = n - \mu_{nl}$ ($n \geqslant n_0$) is the effective principal quantum number and μ_{nl} are the corresponding quantum defects. To a good approximation μ_{nl} is for a particular alkali metal a function of l only (see, e.g., Table 8.1 in Ref. [9]). Then the binding energy of the valence electron in the lowest state, i.e., the ionization potential of the atom, is $I_p = 1/2n^{*2}$, where the effective principal quantum number n^* in this case corresponds to the orbital $n_0 s$.

Using the single-electron picture (valence electron plus atomic core), we study here the alkali-metal atoms under the influence of a quasistatic electric field. We assume further that the field effects on the core electrons can be neglected. Obviously such a frozen-core approximation (FCA) is valid if the mutual interaction of the core electrons and their interaction with the nucleus are much stronger than the interaction between these electrons and the field. This requirement is fulfilled if the field is not extremely strong. In addition, even if a polarization of the core due to an external field is noticeable, it becomes unimportant when the valence electron separates from the core because in this case their interaction reduces to the pure Coulomb interaction between two point charges. Compared to the interactions inside the core, the interaction between the core and the valence electron, as mentioned above, is much weaker. Moreover, this interaction gradually decreases when the electron, during the ionization process, separates from the core. The dynamics of the valence electron is therefore adequately described if both the interaction with the core and the interaction with the external field are taken into account.

Thus, the potential energy and Hamiltonian of the valence electron of an alkali-metal atom in a (quasi)static electric field F within the FCA read

$$V(\mathbf{r}) = V_{\rm core}(r) - Fz, \quad H = \frac{p^2}{2} + V(\mathbf{r}). \tag{2}$$

The core potential and the external electric field form the potential barrier (the so-called Stark saddle), the saddle point of which lies below the (first) ionization threshold of the free atom [see Figs. 1(b) and 1(c)]. For any $F \neq 0$ at the outer side of the barrier there is a position along the field (i.e., z) axis beyond which the total potential $V(\mathbf{r})$ lies below the binding energy. Since the electron can tunnel through the barrier, the atom has a small but nonzero probability of ionizing, even when the saddle point is well above the bound state. Thus, all states of the system described by the Hamiltonian (2) have the resonant character. We shall consider here the lowest resonance.

The barrier saddle point is located on the z axis at the position $z = z_{\rm SP}$, which depends on the field strength and can be determined from the rule $(\partial V/\partial z)_{x=y=0} = 0$. If the core potential $V_{\rm core}(r)$ for $r \geqslant |z_{\rm SP}|$ can be approximated by the pure Coulomb potential $V_C = -1/r$ one obtains $z_{\rm SP} = 1/\sqrt{F}$ and $V_{\rm SP} \equiv V(\mathbf{r}_{\rm SP}) = -2\sqrt{F}$. The required condition is fulfilled for weak fields ($F \ll 1$) because in this case $z_{\rm SP} \gg 1$ and for $r \gg 1$ the short-range terms in $V_{\rm core}(r)$ vanish.

B. Ionization regimes and Stark shift

If the field is not extremely strong the energy of the lowest state $E(F)$ lies below the saddle point of the barrier [see Fig. 1(b)] and, as mentioned above, the electron can ionize by tunneling through the barrier. By increasing the field the saddle point shifts down and for the strengths larger than a specific value F_s it is suppressed below the energy $E(F)$ [see Fig. 1(c)]. Then the electron escapes over the barrier. Note that from the quantum mechanical point of view there is not an essential difference between these two kinds of ionization processes. However, in the semiclassical approach the tunneling and OBI are treated in different ways.

The value of the field strength $F = F_s$ that separates the tunneling and OBI regimes is defined by equality $E(F) = V_{\rm SP}(F)$. These values for alkali-metal atoms are sufficiently small that the core potentials at distances $r = |z_{\rm SP}(F_s)|$ can be well approximated by the pure Coulomb potential [see Figs. 1(b) and 1(c)]. This is explicitly checked for the ECP models used in this paper (see Sec. III A). Therefore, for alkali-metal atoms F_s can be obtained as the solution of the

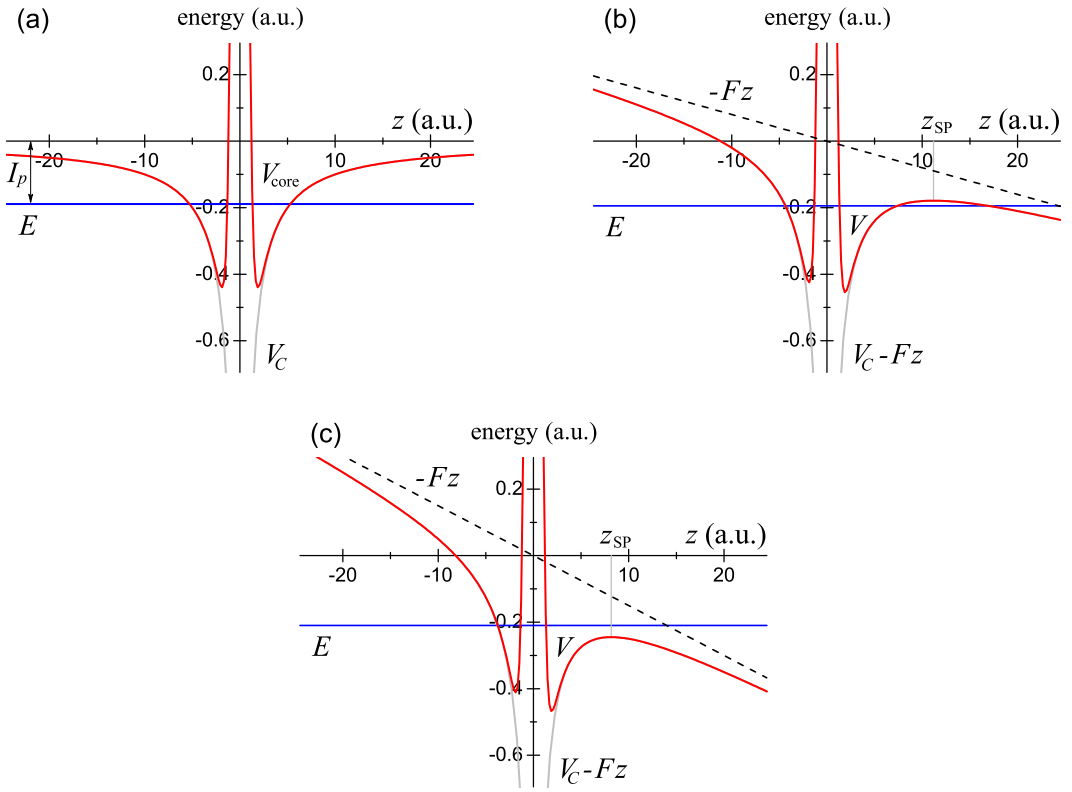

FIG. 1. (Color online) Potential energy $V = V_{\text{core}}(r) - Fz$, i.e., its $x = y = 0$ cut (red lines), and the lowest energy level E (blue lines) of the valence electron of sodium atom for three different strengths of applied electric field: (a) $F = 0$, (b) $F = 0.008$, and (c) $F = 0.015$ a.u. The effective core potential $V_{\text{core}}(r)$ is represented by the Hellmann pseudopotential (8). Cases (b) and (c) correspond to the tunneling and OBI regimes, respectively. For comparison, the sums (gray lines) of the Coulomb potential $V_C = -1/r$ and the corresponding field contributions $-Fz$ (dashed lines) are shown in the same graphs.

equation

$$E(F) = -2\sqrt{F}, \tag{3}$$

which does not depend on the ECP model. Here F_s values can be roughly estimated by taking $E(E) \approx E(0) = -I_p$, which gives $F_s \approx I_p^2/4$.

More accurate values for F_s can be obtained by taking into account the Stark shift of the lowest-energy level, which is the change in the total energy of a neutral atom due to an applied electric field. For $F \ll 1$ the Stark shift can be expanded in a Maclaurin series $\Delta E = -\alpha F^2/2! - \gamma F^4/4! - \cdots$, where the first two coefficients α and γ are known as the dipole polarizability and the second dipole hyperpolarizability, respectively. Within the single-electron model and the FCA one has $\Delta E(F) = E(F) - E(0) = E(F) + I_p$. Thus, the lowest energy of the valence electron at weak fields ($F \ll 1$) can be approximately determined using the fourth-order formula

$$E(F) = -I_p - \tfrac{1}{2}\alpha F^2 - \tfrac{1}{24}\gamma F^4. \tag{4}$$

The values for α and γ are in principle larger for atoms with smaller ionization potentials. The corresponding values for alkali-metal atoms are given in the third and fourth columns of Table I. We have tried to select here the most recent experimental values for the polarizabilities (see Ref. [11] and references therein). The data for francium are missing and for this atom we roughly estimated α and γ from our numerical results. Experimental data for the hyperpolarizabilities are also unavailable and for the remaining five alkali-metal atoms we present the recommended theoretical values [12]. In the same table the F_s values, obtained by solving Eq. (3) with the expansion (4), are given in the fifth column. One can see that for alkali-metal atoms, because of small ionization potentials, the values F_s are much lower than in the case of hydrogen. Consequently, the tunneling regime is for these atoms reduced to a domain of very weak fields. On the other hand, due to large values for the polarizability and hyperpolarizability, the Stark shift of the lowest-energy level for alkali-metal atoms changes with F much faster than for hydrogen (see Fig. 2).

TABLE I. Values for the ionization potential I_p [10], the dipole polarizability α (experimental values) [11], hyperpolarizability γ [12], and the electric field F_s dividing the tunneling and over-the-barrier ionization regimes for hydrogen and alkali-metal atoms (in atomic units).

Atom	I_p	α	γ	F_s
H	0.5	4.5	1333.125	0.06517
Li	0.19814	164.2 ± 1.1	$(2.90 \pm 0.09)\times 10^3$	0.01078
Na	0.18886	162.7 ± 0.8	$(9.56 \pm 0.48)\times 10^5$	0.00969
K	0.15952	290.8 ± 1.4	$(3.6 \pm 1.1)\times 10^6$	0.00697
Rb	0.15351	318.8 ± 1.4	$(6.2 \pm 1.9)\times 10^6$	0.00645
Cs	0.14310	401.0 ± 0.6	$(1.1 \pm 0.3)\times 10^7$	0.00562
Fr	0.14967	350 ± 50[a]	$\sim 10^7$[a]	0.00615

[a]Values estimated from numerical results (see Table V).

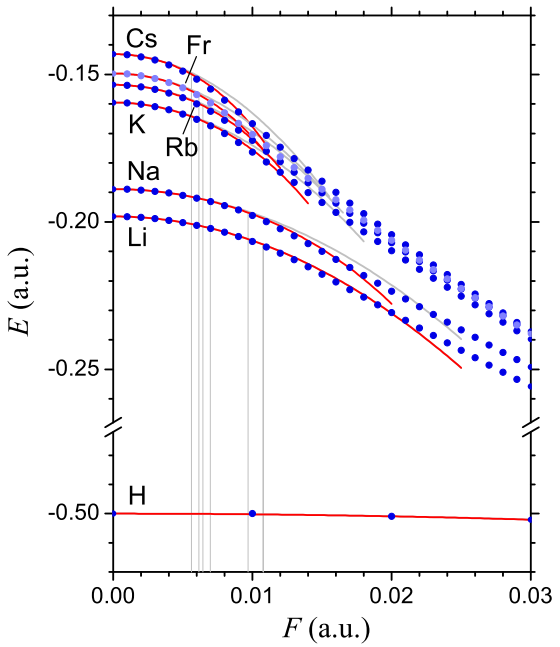

FIG. 2. (Color online) Lowest-energy of alkali-metal atoms versus the electric-field strength F, determined numerically by solving the eigenvalue problem of the Hamiltonian (2) (bullets) and by the use of the expansion (4) up to the second (gray lines) and fourth (red lines) powers of F. For comparison the lowest energy of the hydrogen atom is given at the bottom. Vertical gray lines mark the field strengths F_s dividing the tunneling and OBI areas for each atom.

C. The ADK theory

The ionization rates of atoms in an alternating electric field for the field strengths corresponding to the tunneling regime are given approximately by the ADK formula [4]. This formula is essentially a generalization of the Landau-Lifshitz semiclassical formula determining the ionization rate for the hydrogen atom in a static electric field [13]. In principle this rate can be determined by calculating the probability current for electrons emerging from the barrier. In the Landau-Lifshitz approach the electrons' outgoing wave function is approximated by the WKB solution in the region outside the barrier, which is normalized by fitting to the hydrogen field-free ground-state wave function at a matching point inside the barrier. This approach has been also used in the subsequent work extending the WKB approximation both to excited hydrogenic states [14] and to the states of nonhydrogenic atoms (ADK formula). In the latter case the extension is done by introducing a quantum defect that changes the quantum numbers to nonintegers (effective quantum numbers).

In the case of alkali-metal atoms in their ground states the valence electron is characterized by the orbital quantum number $l = 0$ and the general ADK formula (the variant for static fields) reduces to

$$w = |C_{n^*0}|^2 I_p \left(\frac{2F_0}{F}\right)^{2n^*-1} e^{-2F_0/3F}, \tag{5}$$

where $n^* = 1/\sqrt{2I_p}$ is the effective principal quantum number (the ground-state value), $F_0 = (2I_p)^{3/2}$, and $|C_{n^*0}|^2 = 2^{2n^*}/n^*\Gamma(n^*+1)\Gamma(n^*)$.

If the Keldysh parameter γ is much smaller than one, the results obtained for the static electric field can be extended to the case of a linearly polarized alternating field of the frequency ω applying the transformation $F \to F\cos\omega t$ and averaging over the period $T = 2\pi/\omega$. As a result one has the relation between the ionization rates for the static and the alternating field

$$w_{\rm alt}(F) = \sqrt{\frac{3F}{\pi F_0}}\, w(F), \tag{6}$$

where F is now the peak value of the alternating electric field and $w(F)$ is the corresponding static field rate.

It should be mentioned that the main failure in the ADK theory is not due to the semiclassical (WKB) approximation but to the field-free bound-state wave function used in the matching procedure. A field-related correction to the matching wave function may therefore improve the accuracy of the semiclassical approach. The effect of the field on the bound state is twofold: The field (i) shifts the energy of the field-free state (Stark shift) and (ii) changes the shape and amplitude of the wave function. In contrast to a correction of the wave function, the Stark shift can be easily taken into account by substituting the shifted energy in the zeroth-order rate formula. Of course, the best improvement would be obtained if the corrections (i) and (ii) are included simultaneously (as done in the case of hydrogen atom [15,16]).

For weak fields ($F \ll F_s$) the above-mentioned corrections are usually small and the ADK formula in the original form may be satisfactory. In the case of alkali-metal atoms, however, the absolute value of the Stark shift grows fast with F and the correction (i) seems to be necessary even for weak fields. Accordingly, we can expect that the rate formula (5) will be significantly improved after the replacement

$$I_p \to -E(F) = I_p - \Delta E(F). \tag{7}$$

The easiest way to do this is to use the expansion (4) and the corresponding values for α and γ from Table I. We remark that the replacement (7) must be performed while consistently keeping in mind that the parameters n^* and F_0 depend on I_p. The accuracy of the rate formula (5) with the correction (7) is analyzed in Sec. IV by comparing the obtained ionization rates with numerical results.

III. NUMERICAL METHOD

A. The ECP models

Effective core potentials for alkali-metal atoms can be given in a more or less simple form with parameters that are chosen so that the eigenvalues of the single-electron Hamiltonian with this (pseudo)potential reproduces closely the observed atomic spectrum. Such a pseudopotential in principle contains several terms, including the Coulomb and short-range terms required. The form of the latter must be chosen to be small outside the core. The applicability of pseudopotentials is based on the assumption (following from the quantum defect theory [17]) that one obtains accurate approximations to the valence wave functions outside the core if the effective potential leads to good energies for all the members of each Rydberg series.

TABLE II. Parameters A and a for the Hellmann pseudopotential for alkali-metal atoms and the calculated values of binding energies for the lowest two excited states $-E_{1p}^{\rm calc}$ and $-E_{2s}^{\rm calc}$ (in atomic units). Also shown are the related experimental values $-E_{n_0p}^{\rm expt}$ and $-E_{(n_0+1)s}^{\rm expt}$ [10,21–23] (n_0 is the lowest value of the principal quantum number of the valence electron) and the relative deviations of calculated values from the experimental ones.

Atom	A	a	$-E_{1p}^{\rm calc}$	$-E_{2s}^{\rm calc}$	n_0	$-E_{n_0p}^{\rm expt}$	$-E_{(n_0+1)s}^{\rm expt}$	δ_{1p}	δ_{2s}
Li	34	3.14331	0.11464	0.07418	2	0.13023	0.07418	−12%	0%
Na	21	2.54920	0.11242	0.07210	3	0.11160	0.07158	0.7%	0.7%
K	6.5	1.34523	0.10302	0.06543	4	0.10035	0.06371	2.7%	2.7%
Rb	4.5	1.09993	0.10009	0.06426	5	0.09620	0.06178	4.0%	4.0%
Cs	4.6	1.00340	0.09654	0.06145	6	0.09217	0.05865	4.8%	4.8%
Fr	5.1	1.11600	0.09918	0.06309	7	0.09391	0.05976	5.6%	5.6%

One of the simplest ECP models applicable for alkali-metal atoms is the Hellmann pseudopotential [18] [see Fig. 1(a)]

$$V_{\rm core}(r) = -\frac{1}{r} + \frac{A}{r}e^{-ar}. \tag{8}$$

This effective potential belongs to the class of local pseudopotentials because it acts on each wave function in the same way. The short-range term is represented by the screened Coulomb potential with adjustable parameters A and a. Obviously, the pseudopotential (8) reduces to the pure Coulomb term $-1/r$ when the valence electron is far ($r \to \infty$) from the atomic core [see Fig. 1(a)]. The parameters A and a for a given atom are not uniquely determined and one can find in the literature various values proposed by different authors [19,20]. This is a consequence of the fact that the shape of this pseudopotential is almost insensitive to the variation of one of the parameters if the other is simultaneously adjusted to reproduce always the same ionization potential. The values we use here (see Table II) are chosen so that the potential $V_{\rm core}(r)$ for a given atom reproduces exactly the binding energy of the valence electron in the ground state, i.e., the ionization potential I_p (see Table I) and, in addition, as close as possible the corresponding energies for the lowest two excited states [core]n_0p and [core]$(n_0+1)s$ (see Table II). The corresponding calculated levels are here denoted by $E_{1p}^{\rm calc}$ and $E_{2s}^{\rm calc}$, because in the spectrum obtained using a pseudopotential there are no eigenenergies corresponding to the core orbitals. Note that one can obtain good s and p energies with this pseudopotential only for medium-sized atoms. Particularly for lithium it is not possible to find a set of parameters providing sufficiently good agreement with experimental values for s and p states simultaneously. In this case, since the accuracy of the ionization potential is crucial, the parameters are chosen to get the best agreement for s states.

More accurate ECP models are in principle nonlocal. The parameters in the short-range term of such an ECP take different values when it acts on different states. These pseudopotentials may include, besides the Coulomb and short-range terms, also some multipole terms. Such a pseudopotential for alkali-metal atoms proposed by Bardsley reads [24]

$$V_{\rm core}(r) = -\frac{1}{r} - \frac{\alpha_d}{2(d^2+r^2)^2} - \frac{\alpha_q}{2(d^2+r^2)^3} + V_{\rm SR}(r), \tag{9}$$

where

$$V_{\rm SR}(r) = \sum_l V_{\rm SR}^l(r)|l\rangle\langle l| \tag{10}$$

and $V_{\rm SR}^l(r) = A_l \exp(-\zeta_l r)/r$ are the terms of the short-range potential corresponding to different values of the orbital quantum number l. The values for the dipole and quadrupole polarizabilities of the core α_d and α_q, the cutoff parameter d (approximately equal to the radius of the core), and the parameters A_l and ζ_l are given in Ref. [24] for lithium and sodium. In each case the parameters A_l and ζ_l are chosen so that the two lowest levels of each series are reproduced exactly.

We expect, however, that good results for ionization rates of alkali-metal atoms in an electric field can be obtained using a local pseudopotential, e.g. the Hellmann one. This expectation, as well as the applicability of the FCA in this problem, is based on the fact that the ionization rate depends mainly on the form of potential barrier, which is for weak-field strengths (tunneling regime) almost independent of the shape of the core potential. In order to check this, in the next section we compare the results for lithium and sodium obtained by the use of the two alternative pseudopotentials.

B. Complex rotation method

As we have seen in Sec. II, when the atom is placed in an electric field all the states become resonances. The ionization rate (probability per unit time) from a given state is then proportional to the resonance width $w = \Gamma/\hbar$ (hereafter we set $\hbar = 1$). In this paper we study the field ionization from the atomic ground state.

In principle a resonant state $\psi(\mathbf{r})$ is an eigensolution of the Schrödinger equation that is not square integrable because it asymptotically behaves as a purely outgoing wave and corresponds to a complex eigenenergy $E_{\rm res}$. This energy is related to a pole of the scattering matrix and its real and imaginary parts determine the energy (position) and the width of the resonance $E = {\rm Re}(E_{\rm res})$ and $\Gamma = -2\,{\rm Im}(E_{\rm res})$. The basic idea of the complex rotation method (see, e.g., Ref. [25]) is to make the resonance wave function $\psi(\mathbf{r})$ square integrable by a complex rotation of the coordinate $\psi(\mathbf{r}) \to \psi_\theta(\mathbf{r}) = \psi(e^{i\theta}\mathbf{r})$, where θ is a real parameter called the rotation angle. Such a rotated state $\psi_\theta(\mathbf{r})$ is an eigenfunction of the so-called complex rotated Hamiltonian H_θ obtained from

TABLE III. Lowest-state energies E and widths Γ of lithium at different strengths of applied electric field F, obtained by the complex rotation calculations within the single-electron picture. The calculations are performed separately for the Hellmann and Bardsley ECPs [see Eqs. (8) and (9) and related text].

	Hellmann ECP		Bardsley ECP	
F	E	Γ	E	Γ
0.000	−0.19814	0	−0.19814	0
0.001	−0.19821		−0.19824	
0.002	−0.19842		−0.19849	
0.003	−0.19876		−0.19891	
0.004	−0.19925		−0.19949	
0.005	−0.19989		−0.20023	
0.006	−0.20067		−0.20115	
0.007	−0.20161	4.836×10^{-7}	−0.20224	
0.008	−0.20271	3.179×10^{-6}	−0.20350	3.002×10^{-6}
0.009	−0.20400	2.203×10^{-5}	−0.20496	2.065×10^{-5}
0.010	−0.20549	9.628×10^{-5}	−0.20662	8.965×10^{-5}
0.011	−0.20721	2.967×10^{-4}	−0.20850	2.745×10^{-4}
0.012	−0.20913	7.150×10^{-4}	−0.21059	6.573×10^{-4}
0.013	−0.21123	1.431×10^{-3}	−0.21285	1.309×10^{-3}
0.014	−0.21348	2.481×10^{-3}	−0.21525	2.264×10^{-3}
0.015	−0.21583	3.883×10^{-3}	−0.21775	3.538×10^{-3}
0.016	−0.21824	5.633×10^{-3}	−0.22031	5.114×10^{-3}
0.017	−0.22070	7.684×10^{-3}	−0.22293	6.961×10^{-3}
0.018	−0.22317	0.01001	−0.22553	9.064×10^{-3}
0.019	−0.22565	0.01258	−0.22814	0.01138
0.020	−0.22813	0.01538	−0.23076	0.01391
0.021	−0.23060	0.01837	−0.23336	0.01660
0.022	−0.23305	0.02153	−0.23597	0.01944
0.023	−0.23549	0.02484	−0.23851	0.02243
0.024	−0.23790	0.02827	−0.24105	0.02555
0.025	−0.24030	0.03183	−0.24356	0.02873
0.026	−0.24268	0.03548	−0.24604	0.03199
0.027	−0.24504	0.03925	−0.24852	0.03533
0.028	−0.24738	0.04306	−0.25093	0.03876
0.029	−0.24970	0.04696	−0.25335	0.04222
0.030	−0.25200	0.05094	−0.25574	0.04578

TABLE IV. Lowest-state energies E and widths Γ of sodium at different strengths of applied electric field F, obtained by the complex rotation calculations within the single-electron picture. The calculations are performed separately for the Hellmann and Bardsley ECPs [see Eqs. (8) and (9) and related text].

	Hellmann ECP		Bardsley ECP	
F	E	Γ	E	Γ
0.000	−0.18886	0	−0.18886	0
0.001	−0.18894		−0.18895	
0.002	−0.18919		−0.18920	
0.003	−0.18961		−0.18962	
0.004	−0.19020		−0.19021	
0.005	−0.19096		−0.19098	
0.006	−0.19190		−0.19193	
0.007	−0.19303	1.276×10^{-6}	−0.19307	
0.008	−0.19437	1.279×10^{-5}	−0.19442	1.382×10^{-5}
0.009	−0.19595	7.426×10^{-5}	−0.19598	7.464×10^{-5}
0.010	−0.19778	2.684×10^{-4}	−0.19783	2.695×10^{-4}
0.011	−0.19986	7.097×10^{-4}	−0.19993	7.131×10^{-4}
0.012	−0.20215	1.503×10^{-3}	−0.20229	1.511×10^{-3}
0.013	−0.20461	2.691×10^{-3}	−0.20477	2.712×10^{-3}
0.014	−0.20717	4.287×10^{-3}	−0.20739	4.321×10^{-3}
0.015	−0.20979	6.261×10^{-3}	−0.20998	6.307×10^{-3}
0.016	−0.21245	8.577×10^{-3}	−0.21269	8.633×10^{-3}
0.017	−0.21513	0.01120	−0.21540	0.01127
0.018	−0.21780	0.01409	−0.21811	0.01415
0.019	−0.22047	0.01721	−0.22080	0.01730
0.020	−0.22312	0.02051	−0.22347	0.02061
0.021	−0.22575	0.02400	−0.22614	0.02411
0.022	−0.22836	0.02763	−0.22878	0.02776
0.023	−0.23094	0.03139	−0.23141	0.03155
0.024	−0.23351	0.03527	−0.23401	0.03545
0.025	−0.23605	0.03928	−0.23659	0.03943
0.026	−0.23856	0.04331	−0.23915	0.04349
0.027	−0.24106	0.04745	−0.24170	0.04762
0.028	−0.24353	0.05166	−0.24420	0.05182
0.029	−0.24598	0.05595	−0.24671	0.05607
0.030	−0.24841	0.06025	−0.24920	0.06037

the original Hamiltonian H by the transformations

$$\mathbf{r} \to e^{i\theta}\mathbf{r}, \quad \mathbf{p} \to e^{-i\theta}\mathbf{p}. \tag{11}$$

The rotated Hamiltonian H_θ is a non-Hermitian operator, whose spectrum is in general complex, depends on the rotation angle θ, and has the following properties [25]: (i) The bound (discrete) spectra of H_θ and H coincide, (ii) the continua are rotated by the angle 2θ into the lower complex energy half plane, and (iii) the resonances of H coincide with the complex eigenvalues of H_θ.

The spectrum of the Hamiltonian (2) can be computed by diagonalizing the corresponding rotated Hamiltonian with a properly tuned parameter θ in a square integrable basis that must be complete in the sense that it covers the continuous part of the spectrum too. Dilating the coordinates and momenta in the Hamiltonian (2) according to Eq. (11), one obtains

$$H_\theta = e^{-2i\theta}\frac{p^2}{2} + V_{\text{core}}(e^{i\theta}r) - e^{i\theta}Fz. \tag{12}$$

To diagonalize this Hamiltonian we use the Sturmian basis [26]

$$\chi^{(k)}_{nlm}(\mathbf{r}) = 2k^{3/2}\sqrt{\frac{(n-l-1)!}{n(n+l)!}}(2kr)^l e^{-kr} \times L^{2l+1}_{n-l-1}(2kr)Y_{lm}(\theta,\phi), \tag{13}$$

where $L^\alpha_n(x)$ are the generalized Laguerre polynomials. The functions (13), the so-called Coulomb Sturmians, are solutions of the equation

$$\left(-\frac{1}{2}\nabla^2 + \frac{k^2}{2} - \frac{nk}{r}\right)\chi^{(k)}_{nlm}(\mathbf{r}) = 0 \tag{14}$$

and obey the potential-weighted orthonormality relation

$$\int d^3\mathbf{r}\, \chi^{(k)*}_{nlm}(\mathbf{r})\frac{1}{r}\chi^{(k)}_{n'l'm'}(\mathbf{r}) = \frac{k}{n}\delta_{nn'}\delta_{ll'}\delta_{mm'}. \tag{15}$$

In this basis the matrix elements of the rotated Hamiltonian (12), both for the Coulomb problem [then instead of $V_{\text{core}}(e^{i\theta}r)$ one has $V_C(e^{i\theta}r) = -e^{-i\theta}Z/r$] and for an ECP problem, either

TABLE V. Lowest-state energies E and widths Γ of potassium, rubidium, cesium, and francium at different strengths of applied electric field F, obtained by the complex rotation calculations within the single-electron picture using the Hellmann pseudopotential (8).

	K		Rb		Cs		Fr	
F	E	Γ	E	Γ	E	Γ	E	Γ
0.000	−0.15952	0	−0.15351	0	−0.14310	0	−0.14967	0
0.001	−0.15967		−0.15368		−0.14333		−0.14986	
0.002	−0.16013		−0.15420		−0.14400		−0.15044	
0.003	−0.16090		−0.15506		−0.14514		−0.15140	
0.004	−0.16199		−0.15629	1.780×10^{-8}	−0.14675	3.258×10^{-7}	−0.15277	6.371×10^{-8}
0.005	−0.16341	6.045×10^{-7}	−0.15790	2.274×10^{-6}	−0.14889	1.923×10^{-5}	−0.15457	5.135×10^{-6}
0.006	−0.16520	1.638×10^{-5}	−0.15995	4.638×10^{-5}	−0.15164	2.350×10^{-4}	−0.15687	8.647×10^{-5}
0.007	−0.16741	1.439×10^{-4}	−0.16250	3.248×10^{-4}	−0.15499	1.092×10^{-3}	−0.15972	5.190×10^{-4}
0.008	−0.17007	6.219×10^{-4}	−0.16552	1.168×10^{-3}	−0.15875	2.903×10^{-3}	−0.16303	1.662×10^{-3}
0.009	−0.17309	1.700×10^{-3}	−0.16887	2.788×10^{-3}	−0.16271	5.655×10^{-3}	−0.16662	3.659×10^{-3}
0.010	−0.17635	3.475×10^{-3}	−0.17239	5.185×10^{-3}	−0.16671	9.181×10^{-3}	−0.17035	6.442×10^{-3}
0.011	−0.17974	5.909×10^{-3}	−0.17598	8.252×10^{-3}	−0.17071	0.01331	−0.17411	9.874×10^{-3}
0.012	−0.18317	8.906×10^{-3}	−0.17958	0.01187	−0.17467	0.01791	−0.17786	0.01382
0.013	−0.18661	0.01237	−0.18316	0.01592	−0.17858	0.02287	−0.18158	0.01818
0.014	−0.19003	0.01621	−0.18670	0.02033	−0.18242	0.02812	−0.18525	0.02287
0.015	−0.19342	0.02036	−0.19020	0.02503	−0.18620	0.03359	−0.18888	0.02781
0.016	−0.19677	0.02477	−0.19365	0.02995	−0.18993	0.03925	−0.19245	0.03297
0.017	−0.20008	0.02938	−0.19706	0.03507	−0.19360	0.04506	−0.19597	0.03829
0.018	−0.20335	0.03416	−0.20042	0.04034	−0.19721	0.05098	−0.19944	0.04376
0.019	−0.20658	0.03909	−0.20373	0.04575	−0.20077	0.05700	−0.20286	0.04934
0.020	−0.20977	0.04414	−0.20701	0.05126	−0.20428	0.06311	−0.20624	0.05502
0.021	−0.21292	0.04929	−0.21024	0.05687	−0.20775	0.06928	−0.20958	0.06078
0.022	−0.21604	0.05452	−0.21343	0.06255	−0.21117	0.07551	−0.21287	0.06660
0.023	−0.21911	0.05983	−0.21658	0.06829	−0.21455	0.08178	−0.21612	0.07249
0.024	−0.22216	0.06520	−0.21969	0.07410	−0.21789	0.08809	−0.21934	0.07841
0.025	−0.22517	0.07062	−0.22278	0.07994	−0.22119	0.09444	−0.22252	0.08438
0.026	−0.22815	0.07608	−0.22583	0.08583	−0.22445	0.10081	−0.22567	0.09038
0.027	−0.23110	0.08158	−0.22884	0.09175	−0.22768	0.10720	−0.22878	0.09641
0.028	−0.23403	0.08711	−0.23183	0.09770	−0.23088	0.11361	−0.23186	0.10246
0.029	−0.23692	0.09267	−0.23479	0.10368	−0.23404	0.12003	−0.23492	0.10853
0.030	−0.23979	0.09825	−0.23772	0.10967	−0.23718	0.12647	−0.23794	0.11462

with the pseudopotential (8) or with (9), can be expressed in analytical forms (see Appendixes A and B).

Due to the nonorthogonality of the basis elements (13) the Schrödinger equation $(H_\theta - E_{\rm res})\psi_\theta = 0$ represented in this basis does not reduce to a typical eigenvalue problem, but rather to a generalized one of the form $(\mathcal{H} - E_{\rm res}S)\mathbf{x} = 0$. The matrices $\mathcal{H}$ and S are given by the matrix elements $\langle\chi^{(k)}_{nlm}|H_\theta|\chi^{(k)}_{n'l'm'}\rangle$ and $\langle\chi^{(k)}_{nlm}|\chi^{(k)}_{n'l'm'}\rangle$, respectively (see Appendixes A and B), whereas the components of the eigenvectors $\mathbf{x}$ are $\langle\chi^{(k)}_{nlm}|\psi_\theta\rangle$. Convergence of the results was ensured by optimizing the Sturmian parameter k and the rotation angle θ. For a large basis [a few tens of states (13)] the resonances only weakly depend on the rotation angle θ. Depending on the field strength, θ here takes the values between 0 and 0.7 rad. Optimizing k is, however, essential ($k \sim 1$). When the parameters are adequately adjusted the computed resonance energies are approximately stationary with respect to variations of these parameters.

IV. RESULTS

The lowest-state energies and widths (ionization rates) for the alkali-metal atoms at different values of applied electric field, obtained numerically by the complex rotation method within the single-electron model, are given in Tables III–V. In order to test the sensitivity of results to the choice of ECP model, the calculations for lithium and sodium are carried out in parallel using the Hellmann and Bardsley pseudopotentials (Tables III and IV). As expected, better agreement between the results for different pseudopotentials is obtained for sodium: The results obtained by the Hellmann pseudopotential in the range $F \in (0,0.03)$ do not deviate by more than 0.3% for energies and 0.8% for widths from the values obtained using the Bardsley pseudopotential. However, even for lithium, i.e., the alkaline-earth element for which the Hellmann pseudopotential poorly reproduced the observed spectrum (see Table II), the deviations for energies and widths in the same range do not exceed 1.5% and 11.3%, respectively. (These deviations in principle grow with F and the maximal values given here in fact correspond to $F = 0.03$.) The results for lithium suggest that the Hellmann pseudopotential, when used for calculating energies and widths of other alkali-metal elements in an electric field (Table V), should give results of a similar or better accuracy.

Numerically calculated lowest-state energies of alkali-metal atoms as functions of F (using the Bardsley

pseudopotential for Li and Na and the Hellman pseudopotential for K, Rb, Cs, and Fr) are shown in Fig. 2 together with the estimations based on the Stark shift expansion (4). The formula that takes into account only the quadratic Stark shift ($\Delta E = -\alpha F^2/2$) agrees with numerical results approximately for $F < F_s$, whereas the application of the full expression (4) (with the fourth-order term) extends the agreement approximately to $F < 1.75F_s$. We remark that the values for polarizabilities given in Table II are experimental data (except for francium), whereas the values for hyperpolarizabilities are estimated from the calculations beyond the single-particle model. Thus, the agreement between the energies $E(F)$ calculated numerically and those obtained by formula (4) (in the domain of validity) confirms the accuracy of the former and consequently confirms the applicability of the single-electron approach and ECP models. It should be

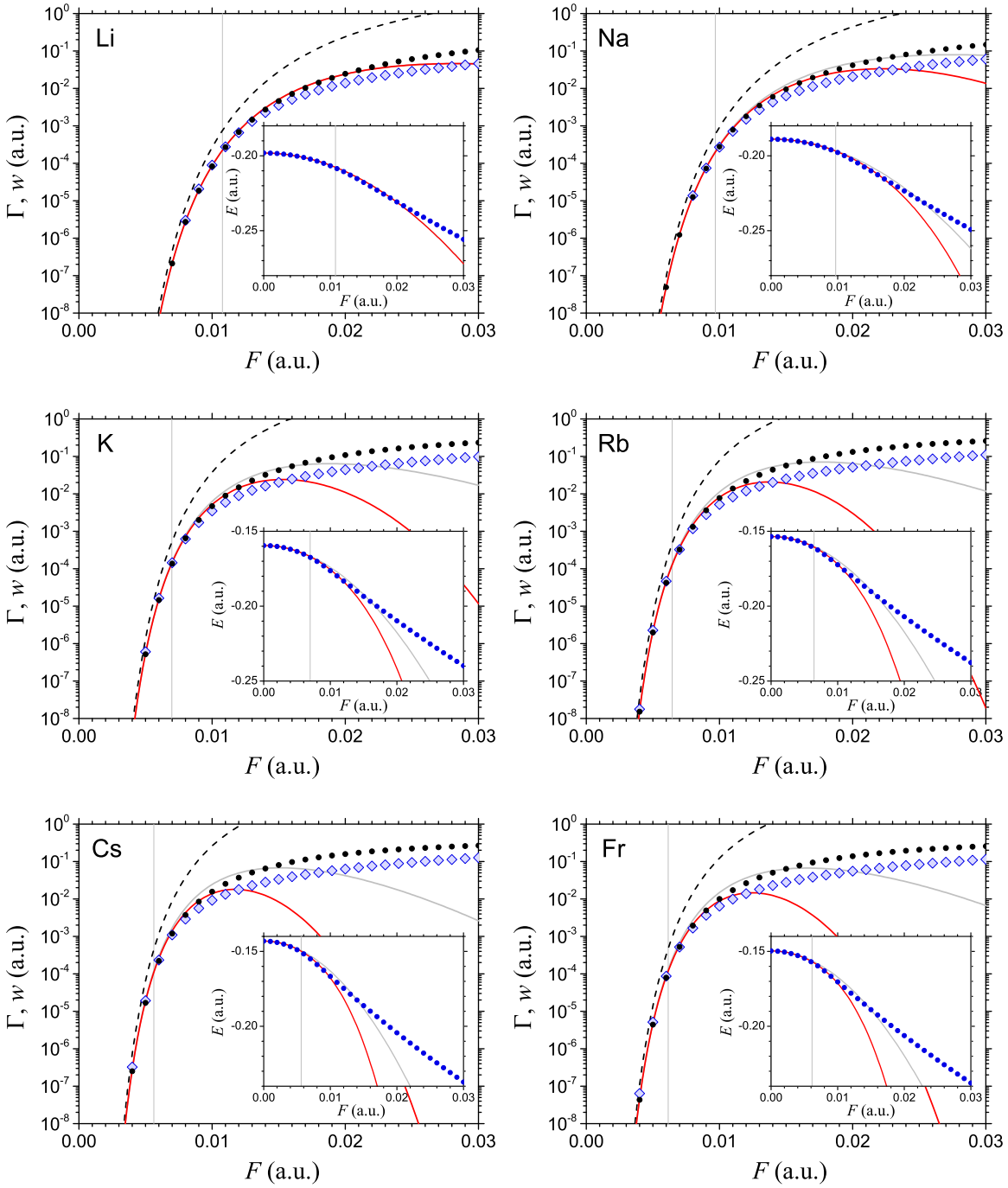

FIG. 3. (Color online) Lowest-state widths and ionization rates of alkali-metal atoms in the static electric field F determined numerically (diamonds), by the ADK formula (dashed lines), by the ADK formula with second- (fourth-) order Stark shift correction [solid gray (red) lines], and by the ADK formula corrected using numerically calculated energy (black dots). The corresponding energies [obtained numerically and by the use of Eq. (4)] are shown in the insets (dots and solid lines, respectively). Vertical gray lines mark the field strengths F_s dividing the tunneling and OBI areas for each atom.

stressed, however, that for field strengths significantly larger than F_s the expansion formula does not converge and the estimated energies strongly deviate from numerical values, which in the OBI regime decrease more linearly.

Numerically calculated widths of the lowest state (the ionization rates) for alkali-metal atoms in an electric field (again using the Bardsley pseudopotential for Li and Na and the Hellman one for K, Rb, Cs, and Fr), as well as those obtained using the ADK formula, are shown in Fig. 3. For all six atoms a significant disagreement between the numerical and the (uncorrected) ADK values is evident, even at weak-field strengths ($F < F_s$). This fact, however, is not surprising. Namely, in Sec. II we pointed out that the accuracy of the ADK formula, in the case of atoms with low ionization potentials, might be unsatisfactory if we ignore the Stark shift. In the same figure we also show the results obtained by applying the correction (7) in the ADK formula (5). The most accurate and the most general correction is obtained by inserting in Eq. (7) the numerically determined values of energy. However, for the practical use it is more convenient to use the expansion (4). In Fig. 3 we show the rate values obtained by the energy-corrected ADK formula using the numerical values as well as the values determined by the expansion (4) up to the second and fourth powers of F. One can see that, in contrast to the ionization rates obtained by Eq. (5) (uncorrected ADK formula), those obtained using the energy-corrected ADK formula are in an excellent agreement with numerical results in the tunneling domain ($F < F_s$).

Finally, the ionization rates for the alkali-metal atoms in the alternating field $w_{\rm alt}$ are obtained from the static rates using relation (6). Figure 4 shows the ionization rates $w_{\rm alt}$ for these atoms versus the laser field intensity I ($I = I_0 F^2$, where F is given in atomic units and $I_0 = 3.509\,45 \times 10^{16}$ W/cm^2 is the atomic unit value for intensity). For the lowest values of the field strength ($F \ll F_s$) the ionization rates are determined by the energy-corrected ADK formula. Otherwise, the numerical values are used.

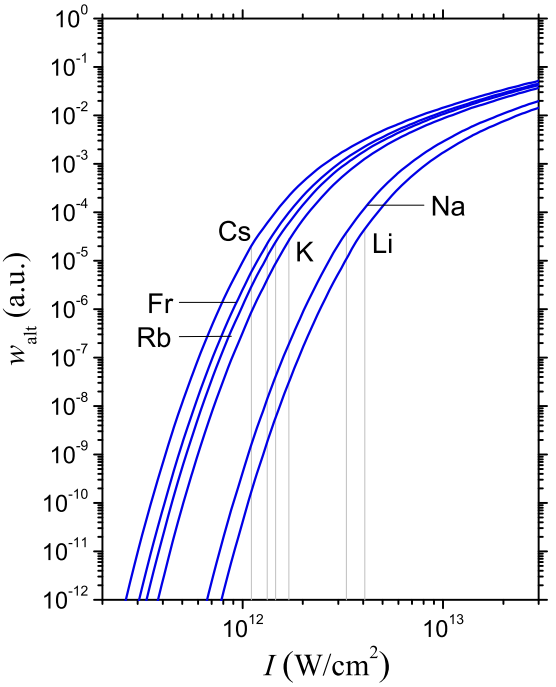

FIG. 4. (Color online) Ionization rates $w_{\rm alt}$ of alkali-metal atoms versus the laser field intensity I. Vertical gray lines mark the field intensities dividing the tunneling and OBI areas for each atom.

V. CONCLUSION

In this paper we studied the alkali-metal atoms in a strong electromagnetic field using the single-electron model (valence electron plus atomic core) and the quasistatic approximation that is applicable when the Keldysh parameter γ [given by Eq. (1)] is much smaller than one. In addition, due to strong interactions inside the core, the field effects on the core electrons can be neglected (the FCA). In this quasistatic field regime the ionization is realized either by the tunneling of the valence electron through or by its escape over the barrier that is formed by the core potential and the external electric field. A consequence of the presence of the barrier is that all states of the atom have resonant character.

The lowest-state energy and the corresponding width, which is proportional to the ionization rate, for the field strengths corresponding to the tunneling regime ($F < F_s$, where F_s is the OBI threshold) were estimated from the Stark shift expansion (4) and from the ADK formula (5), respectively. It was shown that for alkali-metal atoms, because of small ionization potentials, the values F_s are much lower than in the case of hydrogen (see Table I) and the tunneling domain is significantly reduced. On the other hand, when F increases (starting from zero), the lowest-energy levels of alkali-metal atoms, due to large values for the dipole polarizability and hyperpolarizability, decrease much faster than in the case of hydrogen. For these reasons, the accuracy of the original ADK formula in the case of alkali-metal atoms is not satisfactory and we introduced a correction that takes into account the dependence of the binding energy of the valence electron on the field strength [Eq. (7)].

The lowest-state energies and widths (ionization rates) given by the Stark shift expansion and the corrected ADK formula were compared with numerical results obtained by the complex rotation method. Good agreement for both the energies and the widths was found in the tunneling domain ($F < F_s$). In the numerical calculations two kinds of pseudopotentials were used to simulate the ECP: a local one [the Hellmann pseudopotential (8)] and a nonlocal one [the Bardsley pseudopotential (9)]. It was found that the calculated energies agree with the Stark shift formula slightly better when the nonlocal pseudopotential is used.

The good agreement between the numerically calculated lowest-state energies and those estimated from the polarizability and hyperpolarizability data using the Stark shift expansion formula (4) is a confirmation of the validity of the proposed single-electron model (including the chosen ECP models and the FCA), at least in the tunneling regime. The exactness of the model is obviously the lowest in the inner region where the ECP, as an empirically determined part of the total potential, is significantly different from the Coulomb potential (see Fig. 1). Consequently, this model should be even more adequate for calculating the ionization rates than the energies because the latter are primarily determined by the potential in the inner

region, whereas the former depend mainly on the form of the potential barrier, which is only partially determined by the core potential. (This is also a crucial point in the ADK theory.) Hence we expect that the values of calculated ionization rates in the tunneling regime are correct. A confirmation is the agreement between the numerically calculated rates and those determined by the energy-corrected ADK formula, especially when the numerically determined energies are used. This means that the real and imaginary parts of the calculated complex energy (determined by the complex rotation method) are compatible. A more direct verification, however, is missing. Measurements of the tunneling rates for alkali-metal atoms in quasistatic fields carried out so far (see, e.g., Ref. [6]) were able to confirm only roughly their exponential growth when the field strength increases.

Finally, it should be mentioned that the correction in the ADK formula significantly reduces deviations of the ADK rates from those determined numerically even in the OBI regime ($F > F_s$). A difference between numerical results and those obtained by the energy-corrected ADK formula (with numerically determined energies) in this regime (see Fig. 3) can be attributed to a decrease in accuracy of the latter at stronger fields, when, in addition to the correction in the binding energy, a correction of the wave function form in the inner region is required.

ACKNOWLEDGMENTS

This work was supported by the COST Action No. CM1204 (XLIC). N.S.S. acknowledges support from the Ministry of Education, Science and Technological Development of Republic or Serbia under Project No. 171020.

APPENDIX A: MATRIX ELEMENTS FOR THE COULOMB PROBLEM IN AN ELECTRIC FIELD IN THE STURMIAN BASIS

From the orthonormality relation (15) one obtains directly the matrix elements for the Coulomb potential $V_C = -Z/r$,

$$\langle nlm;k|V_C|n'l'm';k\rangle = -Z\frac{k}{n}\delta_{nn'}\delta_{ll'}\delta_{mm'}, \tag{A1}$$

where $|nlm;k\rangle$ are the Sturmian functions $\chi^{(k)}_{nlm}(\mathbf{r})$ written using Dirac notation. Further, it can be shown that

$$\begin{aligned}&\langle nlm;k|n'l'm';k\rangle\\ &\quad=\frac{1}{2}N_{nl}N_{n'l}\frac{(n+l+1)!}{(n-l-1)!}\delta_{ll'}\delta_{mm'}\\ &\qquad\times\left[\frac{n-l-1}{n+l+1}(\delta_{nn'}-\delta_{n,n'+1})+\delta_{nn'}-\delta_{n,n'-1}\right],\end{aligned} \tag{A2}$$

where

$$N_{nl}=\sqrt{\frac{(n-l-1)!}{n(n+l)!}}. \tag{A3}$$

Then, starting from Eq. (14), it follows that the matrix elements for the kinetic energy operator $T = p^2/2 = -\frac{1}{2}\nabla^2$ can be expressed in terms of the matrix elements (A1) for $Z = 1$ and (A2), i.e.,

$$\begin{aligned}&\langle nlm;k|T|n'l'm';k\rangle\\ &\quad=k^2(\delta_{nn'}\delta_{ll'}\delta_{mm'}-\tfrac{1}{2}\langle nlm;k|n'l'm';k\rangle).\end{aligned} \tag{A4}$$

The matrix elements of the field contribution $V_F = -Fz$ to the total potential, after transition to spherical coordinates, can be written in the form of a product of an angular and a radial integral

$$\langle nlm;k|V_F|n'l'm';k\rangle = -FI_a(l,m;l',m')I_r(n,l;n',l'). \tag{A5}$$

The angular integrals are

$$\begin{aligned}I_a(l,m;l',m')=&\frac{1}{\sqrt{(2l+1)(2l'+1)}}\sqrt{\frac{(l+m)!(l'-m)!}{(l-m)!(l'+m)!}}\\&\times[(l+m+1)\delta_{l+1,l'}+(l-m)\delta_{l-1,l'}]\delta_{mm'}.\end{aligned} \tag{A6}$$

Obviously, the nonzero angular integrals are those with $l' = l \pm 1$. Thus, the only radial integrals required here are $I_r(n,l;n',l' = l+1)$ and $I_r(n,l;n',l' = l-1)$. The first integral can be written in the form

$$I_r(n,l;n',l'=l+1)=\frac{N_{nl}N_{n'l'}}{4k}\left(J^{(l)}_{n,n'}-J^{(l)}_{n-1,n'}\right), \tag{A7}$$

where

$$J^{(l)}_{n,n'}=\frac{(n+l+1)!}{(n-l-1)!}(\delta_{n-1,n'}-3\delta_{n,n'}+3\delta_{n+1,n'}-\delta_{n+2,n'}). \tag{A8}$$

The second radial integral reduces to the first one [Eq. (A7)] with exchanged indices (n,l) and (n',l'), i.e., $I_r(n,l;n',l'=l-1)\equiv I_r(n,l=l'+1;n',l')=I_r(n',l';n,l=l'+1)$. Finally, the matrix elements of the rotated Hamiltonian for the Coulomb problem in an electric field are

$$\begin{aligned}&\langle nlm;k|H_\theta|n'l'm';k\rangle\\ &\quad=e^{-2i\theta}\langle nlm;k|T|n'l'm';k\rangle+e^{-i\theta}\langle nlm;k|V_C|n'l'm';k\rangle\\ &\qquad+e^{i\theta}\langle nlm;k|V_F|n'l'm';k\rangle.\end{aligned} \tag{A9}$$

APPENDIX B: PSEUDOPOTENTIAL MATRIX ELEMENTS IN THE STURMIAN BASIS

To construct the matrix elements of the rotated Hamiltonian (12), besides the elements that appear in Eq. (A9), we need also the matrix elements of the non-Coulomb terms in $V_{\rm core}(e^{i\theta}r)$. The Hellmann's pseudopotential (8), in addition to the Coulomb term (with $Z = 1$), contains a short-range term that has the form of the screened Coulomb potential $V_{\rm SR}(r) = Ae^{-ar}/r$. The Bardsley pseudopotential (9), besides the Coulomb term, contains a sum of short-range terms of this kind as well as the dipole and quadrupole terms $V_d(r) = -\frac{1}{2}\alpha_d/(d^2+r^2)^2$ and $V_q(r) = -\frac{1}{2}\alpha_q/(d^2+r^2)^3$, respectively. The matrix elements of the rotated short-range

potential $V_\theta^{\rm SR}(r) \equiv V_{\rm SR}(e^{i\theta}r)$ are

$$\langle nlm;k|V_\theta^{\rm SR}|n'l'm';k\rangle = AN_{nl}N_{n'l}\delta_{ll'}\delta_{mm'}\frac{(n+n'-1)!}{(n-l-1)!(n'-l-1)!}\frac{ke^{-i\theta}x^{2l+2}}{(1+x)^{n+n'}} \times {}_2F_1(l+1-n,l+1-n';1-n-n';1-x^2), \quad \text{(B1)}$$

where $x = e^{-i\theta}2k/a$ and N_{nl} and $N_{n'l}$ are given by Eq. (A3). The matrix elements of the rotated dipole and quadrupole terms $V_\theta^d(r) \equiv V_d(e^{i\theta}r)$ and $V_\theta^q(r) \equiv V_q(e^{i\theta}r)$, respectively, can be expressed as the sums

$$\langle nlm;k|V_\theta^d|n'l'm';k\rangle = \delta_{ll'}\delta_{mm'}N_{nl}N_{n'l}\frac{\alpha_d\xi^{\lambda+2}}{4d^4}\sum_{i=0}^{u}\frac{(-\xi)^i}{i!}\binom{u+\lambda}{u-i} \times \sum_{j=0}^{v}\frac{(-\xi)^j}{j!}\binom{v+\lambda}{v-j}I^{(2)}_{i+j+\lambda+1}(\xi), \quad \text{(B2)}$$

$$\langle nlm;k|V_\theta^q|n'l'm';k\rangle = \delta_{ll'}\delta_{mm'}N_{nl}N_{n'l}\frac{\alpha_q\xi^{\lambda+2}}{4d^6}\sum_{i=0}^{u}\frac{(-\xi)^i}{i!}\binom{u+\lambda}{u-i} \times \sum_{j=0}^{v}\frac{(-\xi)^j}{j!}\binom{v+\lambda}{v-j}I^{(3)}_{i+j+\lambda+1}(\xi), \quad \text{(B3)}$$

where $\xi = e^{-i\theta}2kd$, $\lambda = 2l+1$, $u = n-l-1$, $v = n'-l-1$, and

$$I^{(s)}_\kappa(\xi) = \int_0^\infty \frac{t^\kappa e^{-\xi t}}{(1+t^2)^s}dt. \quad \text{(B4)}$$

The integral in (B4) can be expressed in terms of lower-order integrals. For $s=2$ and the odd values of κ one has

$$I^{(2)}_\kappa(\xi) = \frac{(-1)^{(\kappa+1)/2}}{2}\left\{\left[\frac{\kappa-1}{2}I_{\ln}(\xi)+I^{(1)}_0(\xi)\right]\xi - 1 + \sum_{i=1}^{(\kappa-3)/2}(-1)^i\frac{\kappa-2i-1}{2i}\frac{\Gamma(2i+1)}{\xi^{2i}}\right\}, \quad \text{(B5)}$$

whereas for the even values of κ it is

$$I^{(2)}_\kappa(\xi) = \frac{(-1)^{\kappa/2}}{2}\left\{[I^{(1)}_1(\xi)-(\kappa-1)I_{\rm at}(\xi)]\xi - \sum_{i=1}^{\kappa/2-1}(-1)^i\frac{\kappa-2i}{2i-1}\frac{\Gamma(2i)}{\xi^{2i-1}}\right\}. \quad \text{(B6)}$$

For $s=3$ and the odd values of κ the integral (B4) becomes

$$I^{(3)}_\kappa(\xi) = \frac{(-1)^{(\kappa-1)/2}}{4}\left\{\left[\frac{(\kappa-1)(\kappa-3)}{4}I_{\ln}(\xi) + (\kappa-1)I^{(1)}_0(\xi) - I^{(2)}_0(\xi)\right]\xi - (\kappa-2) + \sum_{i=1}^{(\kappa-5)/2}\frac{(-1)^i}{i}\left(\frac{\kappa-3}{2}-i\right)\left(\frac{\kappa-1}{2}-i\right)\frac{\Gamma(2i+1)}{\xi^{2i}}\right\}, \quad \text{(B7)}$$

whereas for the even values of κ one has

$$I^{(3)}_\kappa(\xi) = \frac{(-1)^{\kappa/2}}{4}\left\{\left[\frac{(\kappa-1)(\kappa-3)}{2}I_{\rm at}(\xi) + \frac{2\kappa-3}{2}I^{(1)}_1(\xi)+I^{(2)}_1(\xi)\right]\xi + \sum_{i=1}^{\kappa/2-2}(-1)^i\frac{(\kappa/2-i-1)(\kappa/2-i)}{i-1/2}\frac{\Gamma(2i)}{\xi^{2i-1}}\right\}. \quad \text{(B8)}$$

The lower-order integrals used in the expressions above are

$$I^{(1)}_0(\xi) = \int_0^\infty \frac{e^{-\xi x}}{1+x^2}dx = \cos\xi[\pi - 2\,{\rm Si}(\xi)]/2 + {\rm Ci}(\xi)\sin\xi, \quad \text{(B9)}$$

$$I^{(1)}_1(\xi) = \int_0^\infty \frac{xe^{-\xi x}}{1+x^2}dx = \{\sin\xi[\pi - 2\,{\rm Si}(\xi)] - 2\,{\rm Ci}(\xi)\cos\xi\}/2, \quad \text{(B10)}$$

$$I^{(2)}_0(\xi) = \int_0^\infty \frac{e^{-\xi x}}{(1+x^2)^2}dx = \frac{1}{4}\{-\xi\cos\xi[\pi - 2\,{\rm Si}(\xi)] + 2 - 2\xi\,{\rm Ci}(\xi)\sin\xi\}, \quad \text{(B11)}$$

$$I_{\ln}(\xi) = \int_0^\infty \ln(1+x^2)e^{-\xi x}dx = \{\sin\xi[\pi - 2\,{\rm Si}(\xi)] - 2\,{\rm Ci}(\xi)\cos\xi\}/\xi, \quad \text{(B12)}$$

$$I_{\rm at}(\xi) = \int_0^\infty \arctan(x)e^{-\xi x}dx = \{\cos\xi[\pi - 2\,{\rm Si}(\xi)] + 2\,{\rm Ci}(\xi)\sin\xi\}/2\xi, \quad \text{(B13)}$$

where ${\rm Si}(x) = \int_0^x \sin t/t\,dt$ and ${\rm Ci}(x) = -\int_x^\infty \cos t/t\,dt$ are the sine and cosine integrals, respectively.

[1] P. Agostini and L. F. DiMauro, Adv. At. Mol. Opt. Phys. **61**, 117 (2012).

[2] L. V. Keldysh, Sov. Phys. JETP **20**, 1307 (1965).

[3] M. Protopapas, C. H. Keitel, and P. L. Knight, Rep. Prog. Phys. **60**, 389 (1997).

[4] M. V. Ammosov, N. B. Delone, and V. P. Krainov, Sov. Phys. JETP **64**, 1191 (1986).

[5] S. Augst, D. D. Meyerhofer, D. Strickland, and S. L. Chin, J. Opt. Soc. Am. B **8**, 858 (1991).

[6] W. Xiong and S. L. Chin, Sov. Phys. JETP **72**, 268 (1991).

[7] A. Scrinzi, M. Geissler, and T. Brabec, Phys. Rev. Lett. **83**, 706 (1999).
[8] J. S. Parker, G. S. J. Armstrong, M. Boca, and K. T. Taylor, J. Phys. B **42**, 134011 (2009).
[9] B. H. Bransden and C. J. Joachain, *Physics of Atoms and Molecules* (Wiley, New York, 1990).
[10] J. E. Sansonetti and W. C. Martin, J. Phys. Chem. Ref. Data **34**, 1559 (2005).
[11] J. Mitroy, M. S. Safronova, and C. W. Clark, J. Phys. B **43**, 202001 (2010).
[12] A. J. Thakkar and C. Lupinetti, in *Atoms, Molecules, and Clusters in Electric Fields: Theoretical Approaches to the Calculation of Electric Polarizability*, edited by George Maroulis (Imperial College Press, London, 2006), p. 505.
[13] L. D. Landau and E. M. Lifshitz, in *Quantum Mechanics* (Pergamon, Oxford, 1991), p. 296.
[14] A. M. Perelomov, V. S. Popov, and M. V. Terent'ev, Sov. Phys. JETP **23**, 924 (1966).
[15] R. J. Damburg and V. V. Kolosov, J. Phys. B **11**, 1921 (1978).
[16] H. J. Silverstone, B. G. Adams, J. Cizek, and P. Otto, Phys. Rev. Lett. **43**, 1498 (1979).
[17] M. J. Seaton, Mon. Not. R. Astron. Soc. **118**, 504 (1958).
[18] H. Hellmann, J. Chem. Phys. **3**, 61 (1935).
[19] G. A. Hart and P. L. Goodfriend, J. Chem. Phys. **53**, 448 (1970).
[20] W. H. E. Schwarz, J. Chem. Phys. **54**, 1842 (1971).
[21] C. E. Moore, *Atomic Energy Levels*, Natl. Bur. Stand. (U.S.) Circ. No. 467 (U.S. GPO, Washington, DC, 1948), Vol. I, Sec. 1.
[22] C. Corliss and J. Sugar, J. Phys. Chem. Ref. Data **8**, 1109 (1979).
[23] U. I. Safronova, W. R. Johnson, and M. S. Safronova, Phys. Rev. A **76**, 042504 (2007).
[24] J. N. Bardsley, Chem. Phys. Lett. **7**, 517 (1970).
[25] A. Buchleitner, B. Grémaud, and D. Delande, J. Phys. B **27**, 2663 (1994).
[26] J. Avery and J. Avery, *Generalized Sturmians and Atomic Spectra* (World Scientific, Singapore, 2006).